SIN-CHN
SCIENTIFIC PRESS PTE.LTD.

*Molecular & Cellular Biomechanics* 2024, 21(1), 260.
https://doi.org/10.62617/mcb.v21i1.260

Article

# Modeling and simulation of nonlinear dynamical systems for biosensor sensitivity based on carbon nanocomposites

**Meng Wang[1], Na Jin[2,*]**

[1] Department of Mathematics and Computer Science, Hetao University, Bayan Nur 015000, China
[2] Physical education department, Hetao University, Bayan Nur 015000, China
*** Corresponding author:** Na Jin, jinna1645@163.com

**CITATION**

Wang M, Jin N. Modeling and simulation of nonlinear dynamical systems for biosensor sensitivity based on carbon nanocomposites. Molecular & Cellular Biomechanics. 2024; 21(1): 260. https://doi.org/10.62617/mcb.v21i1.260

**ARTICLE INFO**

Received: 23 July 2024
Accepted: 4 September 2024
Available online: 9 October 2024



**Abstract:** Nanomaterials have a wide range of applications in various fields of scientific research due to their unique physical and chemical properties. With the rapid development of science and technology, nanocomposites synthesized from various nanoparticles have obtained many excellent properties due to their synergistic effects. In this paper, a series of carbon-based nanomaterials are proposed for in-depth research, and corresponding biosensors are constructed. In this study, ECL biosensors based on a variety of nanocomposite materials will be used to detect and analyze cells, and also detect other cells that are similar to cells. The experimental data show that the relative standard deviation of the detection results of the two methods is within 8%, and the sensor has high sensitivity, excellent stability and fast response speed. The sensor showed excellent performance in the repeatability test, and the relative standard deviation of repeated detection was less than 2%. This result shows that the sensor has highly consistent detection capabilities, providing important support for its reliability in practical applications. By adding the description of repeatability data, the summary more comprehensively reflects the performance advantages of the sensor.

**Keywords:** carbon nanocomposites; biosensor sensitivity; aptamer sensor detection; nonlinear dynamical systems

## 1. Introduction

Biosensors are a cutting-edge research field involving multiple disciplines such as physics, chemistry, biology, and materials science, and have broad application prospects in medical diagnosis, environmental monitoring, food safety, and biomedical engineering. Among them, electrochemical biosensors based on electrochemical sensing technology have become an important research direction in this field due to their high sensitivity, fast response and low cost. With the rapid development of nanotechnology, the performance of electrochemical biosensors has been significantly improved. Especially driven by new nanomaterials, these sensors have demonstrated unprecedented detection capabilities and application potential. In recent years, the scientific and industrial circles have paid increasing attention to nanomaterials. Research on the application of new nanomaterials in biosensors has gradually become a hot topic, creating many new research directions and technological breakthroughs.

As one of the materials with the greatest development potential in the 21st century, nanocomposites have been applied in many fields such as energy, environment, biomedicine and electronics. Compared with traditional materials, nanocomposites have demonstrated outstanding performance advantages due to their nanosize effect, extremely large specific surface area, strong interfacial interactions,

and unique physical and chemical properties. These materials not only break the limitations of traditional materials in terms of structure and function, but also significantly improve their mechanical properties, electrical conductivity, thermal conductivity and catalytic activity through the precise combination of different components and the control of microstructure. The preparation technology of nanocomposites occupies a core position in current nanoscience research. Scientists continue to develop specific nanocomposite materials through various advanced synthesis methods, such as sol-gel method, self-assembly technology, and physical vapor deposition. Functional nanocomposites. The diversity and controllability of these materials provide broad space and unlimited possibilities for future sensor design and development.

The innovations of this paper are reflected in the following aspects: (1) This research not only provides new ideas in the development of new nanomaterials, but also provides theoretical support for improving the detection sensitivity and stability of sensor technology. This article discusses the application of nanocomposites in electrochemical biosensors in detail. Through the optimized design of different material combinations, the sensor performance is significantly improved, laying a foundation for the development of future sensor technology. (2) The modeling and simulation of biosensor sensitivity nonlinear dynamic systems based on carbon nanocomposites demonstrates a brand-new methodology, which is not only innovative in theory, but also shows good operability and practical application. reliability. This paper systematically analyzes the nonlinear response characteristics of sensors and proposes a new modeling framework that can more accurately describe and predict the performance of sensors in complex biological environments. This research result is of great significance to improving the detection accuracy and adaptability of the sensor, and provides a new theoretical basis and technical path for future sensor design.

## 2. Related work

With the development of social economy, more and more scholars have studied carbon nanocomposites. Wang et al. studied the process of preparing silicon carbide refractory from silicon nitride on a nitride binder with high strength, heat resistance and alkali resistance. A large number of silicon powder heating experiments were carried out in nitrogen medium [1]. Bagotia et al. studied toughened polycarbonate (PC) conductive nanocomposites (NCs) prepared by melt blending, the loadings of its multi-walled carbon nanotubes (MWCNTs) range from 0.25 to 10 phr [2]. Liang et al. designed a unique hollow porous bowl-shaped nitrogen-doped cobalt/carbon nanocomposite (HBN-Co/C) to improve electromagnetic microwave absorption (EMA) [3]. Jang et al. incorporated various carbon nanofillers, such as carbon nanotubes, graphene oxide, poly (styrene sulfonate)-wrapped reduced GO, and graphitic nanoplates, which were used to study the effect of nanofiller type and surface treatment on the electrical and rheological properties of polystyrene (PS) nanocomposites prepared by a latex-based process [4]. The results of the Kozlovstudy show that the theoretical model of the polymer micro component cannot describe the change in melt viscosity of polypropylene/spheroidal carbon nanocomposites with changes in nanofiller content [5]. Wang et al. used a robust strategy to prepare N, P

co-doped hollow carbon nanocomposites combined with WSe 2 nanosheets. And the strategy includes metal chelation coordination and high temperature selenization treatment [6]. Li et al. used the semi-crystalline polymer polyacrylonitrile (PAN) and various types of carbon nanomaterials, including $C_{60}$, carbon nanotube (CNT), and graphene oxide (GO). A small-amplitude uniaxial dynamic strain of 0.2% was applied on the prepared nanocomposite films [7]. Pal et al. carried out a detailed investigation by considering a large number of carbon black (CB) samples with particle sizes in the range of 15–65 nm. He used advanced cavity perturbation method (CPM) to measure the dielectric properties of carbon black/epoxy nanocomposites synthesized before and after microwave curing [8]. However, the shortcomings of these studies are that the model construction is not scientific enough and lacks theoretical data support.

## 3. Methods for biosensor sensitivity based on carbon nanocomposites

### 3.1. Application of carbon nanomaterials in biosensors

Carbon is an important non-metallic element. It has many electrons orbital properties (sp, $sp^2$, $sp^3$), resulting in many materials with unique structures and properties. Carbon nanomaterials have been widely and effectively used in the field of biosensors due to their good biocompatibility, catalytic performance, electrical conductivity, large specific surface area, and strong adsorption capacity [9].

(1) Carbon-based materials

Carbon is a very common element with various forms of carbon cores. The two most common types of carbon cores are high-hard diamond with different crystal structures and bond strengths, and soft and smooth graphite. Three-dimensional diamond, layered graphite, two-dimensional graphene, one-dimensional carbon nanotubes, and zero-dimensional fuller spheres constitute a complete carbon family [10]. The summary is as follows (**Figure 1**):

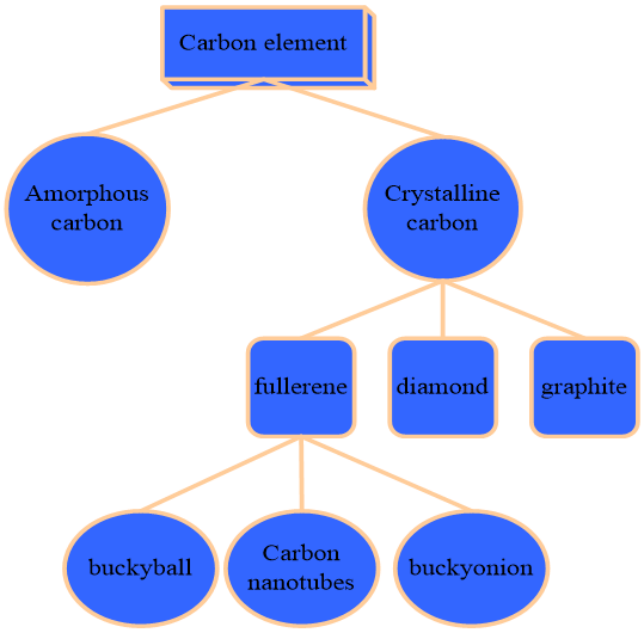


**Figure 1.** Composition diagram of carbon element.

(2) Fullerene

In 1985, a new carbon-$C_{60}$ molecule was discovered in elemental form. It consists of 60 carbon atoms to form a football-like 32-sided body, including 20 hexagons and 12 pentagons. The structure is shown in **Figure 2** [11].

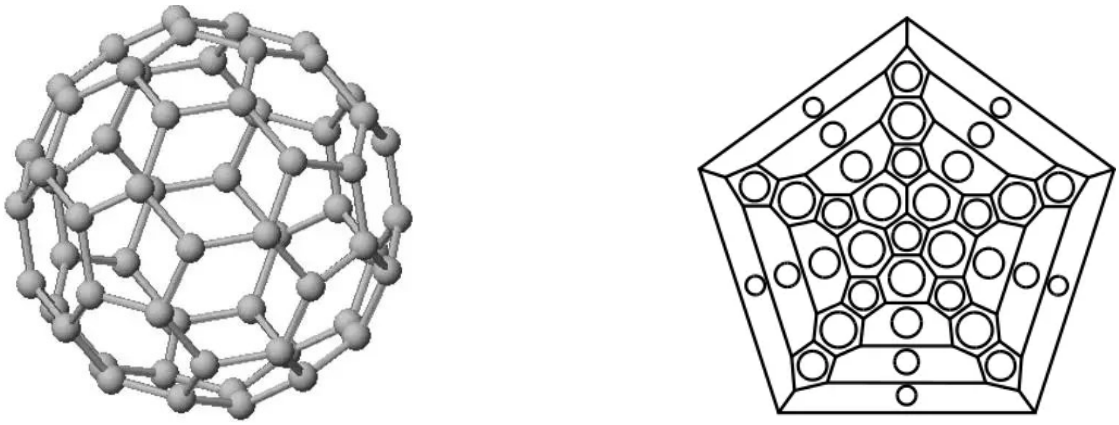

**(a)** **(b)**

**Figure 2.** Schematic diagram of the structure of fullerenes; **(a)** 32-sided body structure; (**b**) pentagonal structure.

Fullerenes can be widely used as a fluorescence quencher in the field of biosensing. For example, a fullerene-based fluorescence sensor was used for Ag+ detection. Through the π-π stacking effect, the probe DNA strands labeled with fluorophores can be adsorbed on the surface of fullerenes, and the fluorescence of the fluorophores is quenched. When Ag+ is added, Ag+ and the probe DNA strand combine to form a rigid structure of "C-Ag-C". The fluorophore is moved away from the fullerene, and the fluorescence is restored. This design enables rapid and sensitive detection of Ag+ [12].

(3) Nanocomposite materials

Nanocomposite is a special kind of composite material. It is a composite material with a dispersion size of at least less than 100 nm. Nanocomposites are not only mixtures of organic and inorganic substances, but also two-phase mixtures of nanoscale and submicron scales. Compared with existing nanomaterials, nanocomposites have better properties and have attracted extensive attention in the scientific community.

However, few single nanomaterials can really be applied to scientific research and fabrication of nanodevices. At present, only a few precious metal nanoparticles, carbon nanotubes and semiconductor nanocrystals have been practically used, and the number is very limited. With the rapid development of modern social economy and technology, it is urgent to develop new nanomaterials to meet the actual needs of scientific research and production. The development of new nanocomposites is an effective way to solve this problem [13].

## 3.2. Biosensors

(1) The concept of biosensor

Biosensors are mainly composed of biological and physical elements that respond to a specified chemical or biological composition. Its working principle is shown in

**Figure 3**. Biosensors are mainly composed of two parts: bio sensitive membrane and transducer [14].

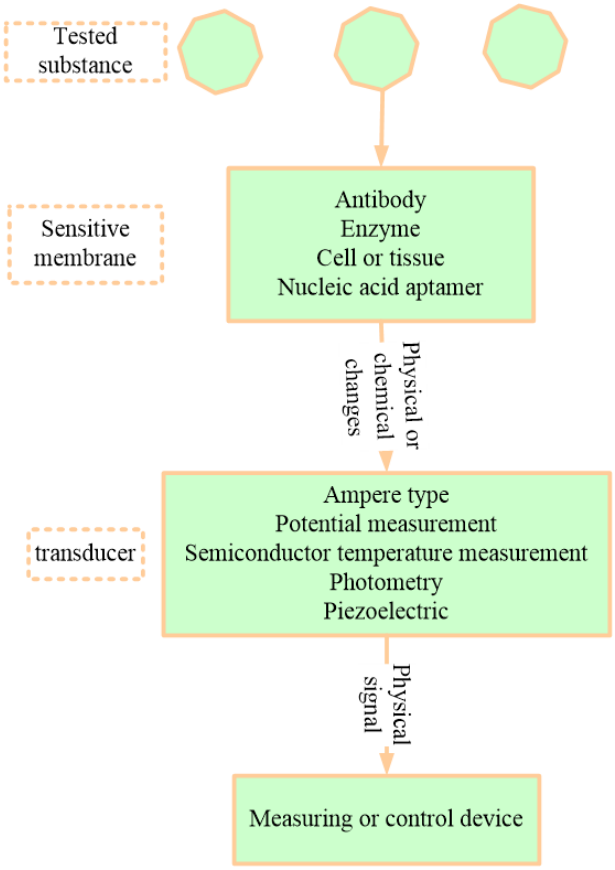


**Figure 3.** Schematic diagram of the biosensor.

(2) Classification of biosensors

The classification of biosensors is shown in **Figure 4**.

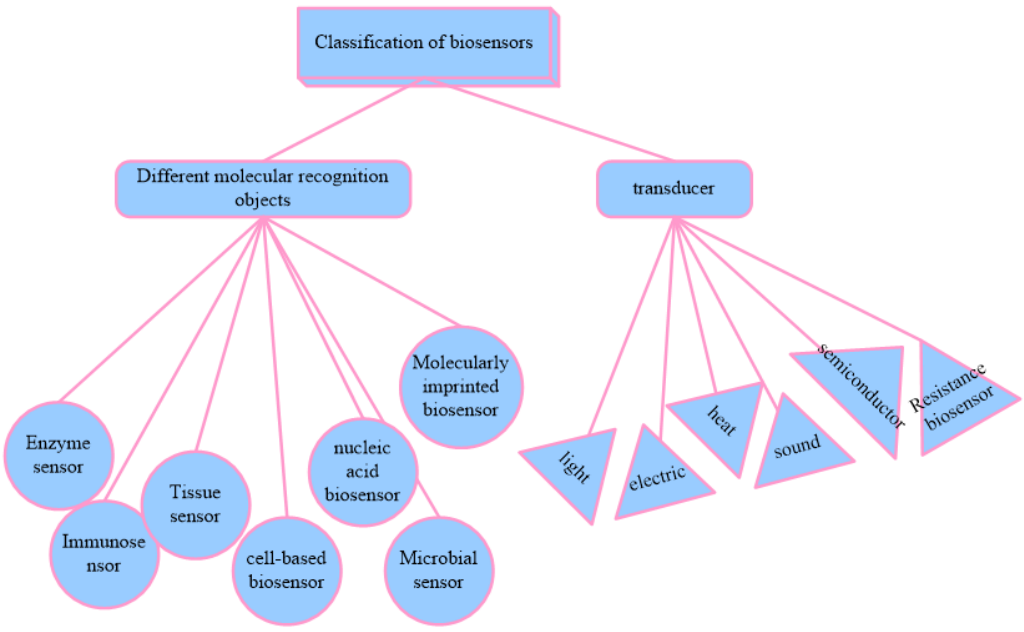


**Figure 4.** Classification of biosensors.

Biosensor is a research field composed of biology, chemistry, physics, electronics and other disciplines [15]. With the application of sensor technology in various fields, it will benefit all mankind.

(3) Detection principle of aptamer sensor

**Figure 5** is a schematic diagram of the detection principle of the aptamer sensor for the measurement substance.

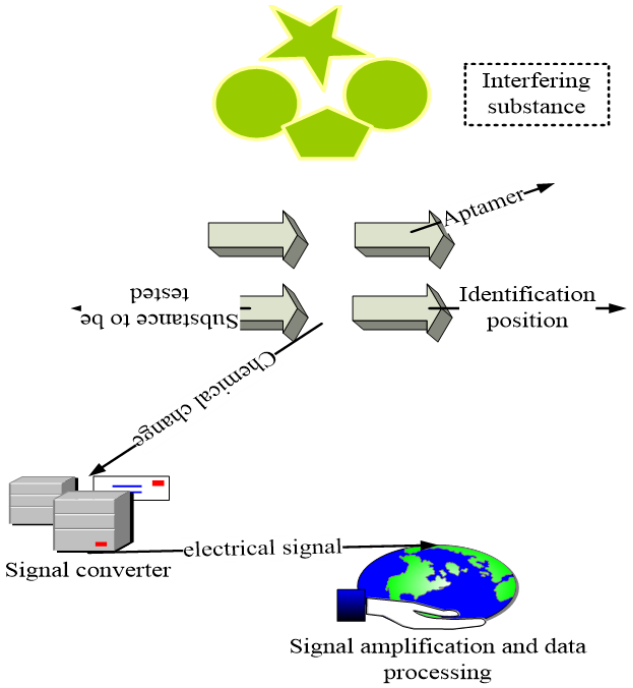


**Figure 5.** Detection principle of the aptamer sensor.

## 3.3. Simulation and calculation of liquid micro-mixing effect based on microfluidic technology

The synthesis of nanomaterials by microfluidic technology is an important application of microfluidic technology. When the chemical reaction is carried out in the microfluidic chip, the concentration, temperature and pressure of the reactants can be precisely regulated. Therefore, the morphology of the reaction product can be well controlled. An understanding of the mixing of fluids in microchannels can also be achieved using computational fluid dynamics simulations [16].

(1) Basic parameters of nanofluids

In order to obtain its mixing effect, some basic parameters and concepts of nanofluids, such as Reynolds coefficient, viscosity and turbulence, are listed below.

1) Reynolds coefficient: Reynolds number ($R_e$)

The Reynolds coefficient is the most important parameter in fluid mechanics, and its specific definition is as follows:

$$R_e = \frac{\chi v d}{\xi} \tag{1}$$

In the equation, $\chi$—the average density of the fluid (kg/m$^3$); $d$—Equivalent diameter of the channel; $\xi$—Hydrodynamic viscosity coefficient (Pa·s).

Here $R_e$ represents the ratio between inertial force and viscous force. In the micro-channels studied in this topic, since $R_e$ is set to be less than 0.01, this value is

compared with the viscous force, and the effect of inertial force can be ignored. At this time, an obvious laminar flow pattern appears [17].

2) Pecklet coefficient ($q_e$)

The Pecklet number is a dimensionless number used to express the relative proportions of convection and diffusion. As the number of $q_e$ decreases, the proportion of diffusive transport increases and the proportion of convective transport decreases, which can be expressed as:

$$q_e = R_e qr = \frac{VH}{\alpha} \tag{2}$$

a) Density and specific heat:

$$\chi_{nf} = (1-\lambda)\chi_{bf} + \lambda\chi_{nq} \tag{3}$$

b) Heat capacity:

$$G_{q,nf} = \frac{(1-\lambda)\chi_{bf}G_{q,bf} + \lambda\chi_{nq}G_{q,nq}}{\chi_{nf}} \tag{4}$$

c) The viscosity of the nanofluid:

$$\frac{\xi_{nf}}{\xi_{bf}} = \frac{1}{1 - 34.87\left(d_{nq}/d_{bf}\right)^{-0.3}\lambda^{1.08}} \tag{5}$$

d) Equivalent diameter of cerium nitrate molecule:

$$d_{bf} = 0.1\left(\frac{6U}{V\pi\chi_{bf0}}\right)^{\frac{1}{3}} \tag{6}$$

3) Shearing force

$$\phi = \frac{F}{B} = \chi \cdot \frac{\mathrm{d}t}{\mathrm{d}y} \tag{7}$$

Among them, $\phi$—shear stress (N/m$^2$), d$t$/d$y$—normal velocity gradient (1/s), $\chi$—proportional coefficient, called viscosity coefficient or dynamic viscosity, referred to as viscosity (Pa·s).

(2) Quantitative analysis method of mixing degree

Due to the difference of each photo taken, such as the influence of external light intensity, different mixing effects in different positions, etc., all the photos taken and the obtained data need to be normalized [18]. As shown in **Figure 6**:

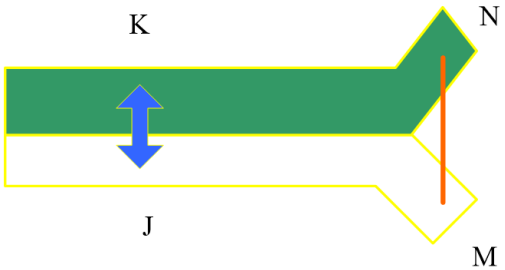


**Figure 6.** Schematic diagram of the normalization process.

The color depth of points M and N is the depth of the solution before micro mixing and can be defined as the highest and lowest depth values (as shown in **Figure 6**). Equation (1) is used to normalize all data on the JK line:

$$A_i = \frac{J_i - J_N}{J_M - J_N} \tag{8}$$

Among them, $A_i$ represents the color depth of each point on the normalized transverse line. $J_i$ represents the measurement of the color depth of each point on the JK line. $J_M$ and $J_N$ represent the color depth measurements of the M and N points. The degree of mixing can be measured by the distribution of the concentration across the cross section of the main channel. The more uniform the concentration distribution, the better the mixing effect. Therefore, standard deviation ($\sigma$) can be used to quantify the distribution of concentrations. If the standard deviation is equal to 0, it means that the two solutions are completely mixed; if it is equal to 0.5, it means that there is no mixing at all [19].

The standard deviation is calculated by the following equation:

$$\sigma = \sqrt{\frac{1}{V-1}\sum_{i=1}^{V}\left(A_i - \overline{A_i}\right)^2} \tag{9}$$

$$\overline{A_i} = \frac{\sum_{i=1}^{v} A_i}{V} \tag{10}$$

Among them, $\sigma$ represents the standard deviation, while $A_i$ represents the normalized color intensity; $\overline{A_i}$ represents the mean intensity. In order to compare the mixing effects of various mixers, this paper defines the mixing percentage $\iota$ to measure the pros and cons of micro-mixers:

$$\iota = 1 - \sigma \tag{11}$$

Among them, $\iota$ is the mixing percentage and $\sigma$ is the standard deviation of the mass fractions in various channels. Since the downstream standard deviation is relatively smaller than the upstream, and the actual situation is that the downstream mixing percentage is larger than the upstream, the difference between Equation (1) and the standard deviation is only the mixing percentage, which can just reflect the pros and cons of the mixing degree [20].

(3) Simulation calculation of liquid micro mixing

The simulation experiment part of the system is completed by using FLUENT software. The Navier-Stokes equations for stable incompressible fluids were applied during the simulation. The specific equation is as follows:

$$\chi\left(\vec{t}\cdot\nabla\right)\vec{t} = \nabla\left[-PI + \xi\left(\nabla\vec{t} + \nabla\vec{t}\right)^K\right] + F \tag{12}$$

$$\nabla\cdot\vec{t} = 0 \tag{13}$$

$$\nabla\cdot\left(-D\nabla G\right) = R - \vec{t}\cdot\nabla G \tag{14}$$

Among them, $\chi$—density (kg/m$^3$), $\vec{t}$—velocity vector (m/s), $P$—pressure (Pa), $\xi$—dynamic viscosity (Pa·s), $F$—Internal force (N/m$^3$), $K$—viscous strength tensor, $D$—diffusion coefficient, $G$—motion scalar, $R$—a source term. Since the simulation process involves two solutions of different properties, the two solutions will diffuse into each other, which is described by the mass transfer equation:

$$\frac{\partial}{\partial k}\left(\chi Y_i\right) + \nabla\cdot\left(\chi\vec{v}Y_i\right) = -\nabla\cdot\vec{H}_i \tag{15}$$

Among them, $\chi$—density (kg/m$^3$), $Y_i$—mass fraction, $\vec{v}$—velocity vector (m/s), $\vec{H}_i$—diffusion flux.

The entire simulation process is carried out in two dimensions, and the remaining relevant parameters of the microchannel are listed in the discussion in each section. The above equation has the following assumptions: (1) There is zero diffusion flux at the sidewall of the microchip. (2) There is no sliding phenomenon or infiltration phenomenon at the side wall of the microchip. (3) The mixing of different aqueous solutions is isotropic at the micron level. (4) Ignore the anisotropy at the micron level. (5) Only a single-phase density exists during the mixing process, ignoring the convection caused by diffusion [21].

### 3.4. BP neural network algorithm

With the continuous development of industrial production and agricultural engineering at the present stage, the objects in control are becoming more and more complex, which requires matching with higher control requirements. The rapid development and application of neural network has made people pay more attention and research on it [22].

According to the designed network, the input and output of each layer can be obtained.

The input and output of the network input layer are:

$$F_T^1 = A(T)(T = 1,2,3,4) \tag{16}$$

The input and output of the hidden layer of the network are:

$$\text{net}_u^2(S) = \sum_T^D K_{uv}^2 F_T^1 \tag{17}$$

$$F_u^2(S) = g\left(net_u^2(S)\right)(u = 1,2,3,4,5) \tag{18}$$

Among them, $K_{\text{uv}}^2$ is the hidden layer weighting coefficient.

The input and output of the network output layer are:

$$\text{net}_L^3(S) = \sum_{u=0}^D K_{uv}^3 F_u^2(S) \tag{19}$$

$$F_L^2(S) = g\left(net_L^3(S)\right)(L = 1,2,3) \tag{20}$$

Among them, (16), (17), (18) are used to represent each layer of the network.

Since this paper studies the direction of chlorination process control, it can be determined that the output of the network is three adjustable parameters $S_q, S_u, S_o$ .And select the activation function of the output layer neurons as a non-negative sigmoid function:

$$F_1^3(S) = S_q \tag{21}$$

$$F_2^3(S) = S_u \tag{22}$$

$$F_3^3(S) = S_o \tag{23}$$

$$P(A) = \frac{e^A}{e^A + e^{-A}} \tag{24}$$

### 3.5. Application of PCR verification technology

To enhance the reliability of the sensor's detection results, this study used polymerase chain reaction (PCR) technology for independent verification. PCR is a molecular biology technique used to amplify and detect specific DNA sequences with

high sensitivity and specificity. The application of this technology in this study includes confirming the gene expression level of the target biomarkers detected by the sensor, thereby verifying the accuracy of the sensor. The experimental steps and result analysis of PCR were compared with the sensor detection data, further demonstrating the universality of the sensor in different cell types and biological samples.

## 4. Performance detection of ECL biosensors based on nanocomposites

The preparation process of the ECL sensor was characterized by electrochemiluminescence properties and electrochemical impedance spectroscopy. For example, when only the cadmium sulfide-modified silica nanocomposite is on the electrode surface, its electrochemiluminescence signal is 3020. When the ionic liquid was modified on the surface of the substrate, the signal intensity increased significantly, reaching 17,340. This is because the ionic liquid contains a large number of free ions, which can realize the transfer and transfer with the ions and electrons in the solution. Therefore, this makes the electrochemiluminescence sensor have a strong signal, which can realize the efficient detection of biological materials. To further modify the antibody onto the electrode surface, 3-aminotrimethoxysilane was used as a bridge. It is able to directly adsorb gold nanoparticles to the electrode surface. However, when human liver cancer antibody was attached to the surface of gold nanoparticles, the signal intensity dropped to about 15,200. This happens because the transfer of electrons is hindered, so the EL signal is reduced. It is through this principle that this biosensor can be fabricated and used to detect liver cancer cells.

### 4.1. Influence of incubation time and pH on immune responses

In order to realize this design for the detection of human hepatoma cells, the detection conditions need to be optimized one by one. The first thing to do is to decide the incubation time of the antibody and cells, as it has a big impact on the detection performance of the sensor. **Figure 7** shows the results obtained from the detection of cells with the same concentration under different incubation time conditions, and the incubation times were 10–50 min. As can be seen from the figure, when the incubation time is 10 min, the electrochemiluminescence signal of the sensor substrate is relatively high, close to the background value. When the incubation time increased to 20 min, it could be seen that the signal intensity of the sensor substrate dropped to about 7500. This indicates that the sensor substrate continues to grow in response to the detected cells as the incubation time increases. As the incubation time increased to 30 min, the electrochemiluminescence signal dropped to around 4000, and when the incubation time continued to increase, the electrochemiluminescence signal of the sensor substrate no longer decreased, but remained relatively stable. It can be seen that 30 min can basically be set as the optimal time for cellular immune binding. Therefore, 30 min was chosen as the optimal incubation time. (The detection solution was a PBS solution (0.1 M, pH 7.4 containing 0.1 M KCl and 0.05 M $K_2S_2O_8$), the scan rate was 100 mV/s, and the PMT voltage was −800 V).

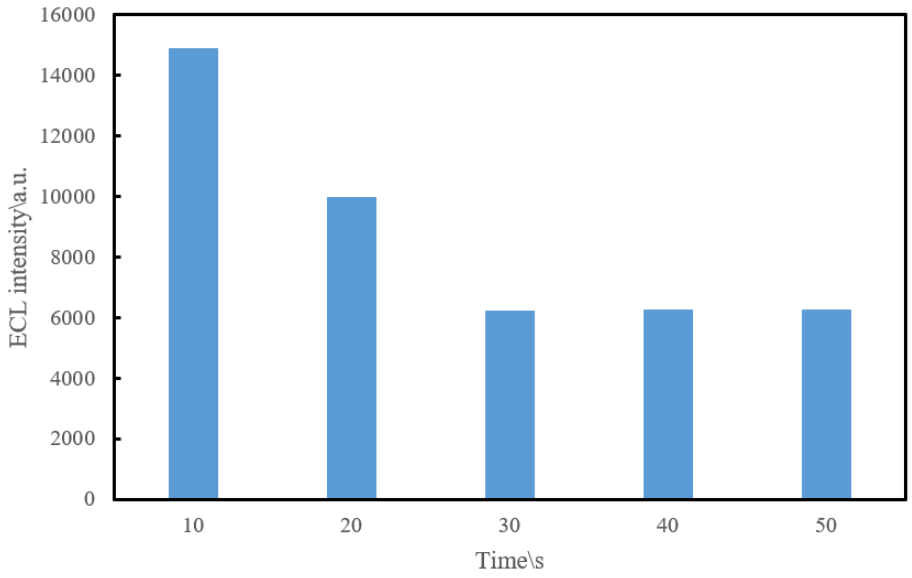


**Figure 7.** ECL-incubation time curve in PBS.

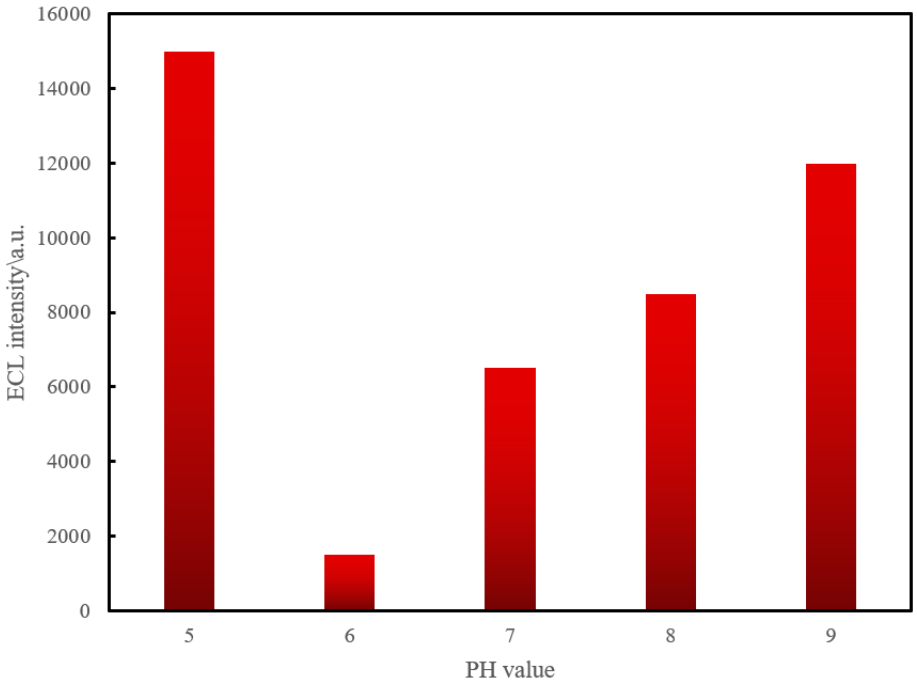


**Figure 8.** Electrochemiluminescence intensity—pH curve.

This paper optimizes the assay performance by changing the pH value and observes the response of antibodies and cells at five different pH values. The experimental approach was performed by observing the responses of antibodies and cells at five different pH values, as shown in **Figure 8**. It can be seen from the results that when the pH value is 5.0, the electrochemiluminescence signal of the sensor substrate is greater than 14,000. With the increase of pH value, the electrochemiluminescence signal of the substrate gradually decreased. Until the pH value was 7.4, the luminescence intensity of ECL decreased to the minimum. This indicates that under these conditions, the binding efficiency of the detected cells and antibodies is the highest. And when the pH value rose above 8.0, the electrochemiluminescence signal of the substrate rose above 13,500. It shows that

under this condition, the binding efficiency between the sensor substrate and the detected cells is relatively low. Therefore, the pH value of 7.4 was selected as the optimum pH value for the entire detection process.

### 4.2. Selectivity, reproducibility and stability of biosensors

It is well known that selectivity, reproducibility and stability are the three most important parameters for a good biosensor. Therefore, for the new sensor designed in this paper, its selectivity should be evaluated first. Due to the similar physical and chemical properties, the assembled cadmium sulfide-modified silica biosensors were then immersed in two cell solutions (5000 cells/mL), respectively. Next, cells attached to the sensor surface without specific binding were removed by careful washing, and the concentration of cells on these biosensors immersed in different cell fluids was measured by electrochemiluminescence. The ECL luminescence intensity of the biosensor immersed in the solution of liver cancer cells was significantly decreased compared with the control cells. However, the silica-cadmium sulfide carrier biosensor that specifically binds to target cells has a good response with cells at a concentration of 300–14,000 cells/mL (**Figure 9**). However, the electrochemiluminescence intensity of the sensor soaked in HeLa cell solution did not change much, which fully reflects the good selectivity of the sensor.

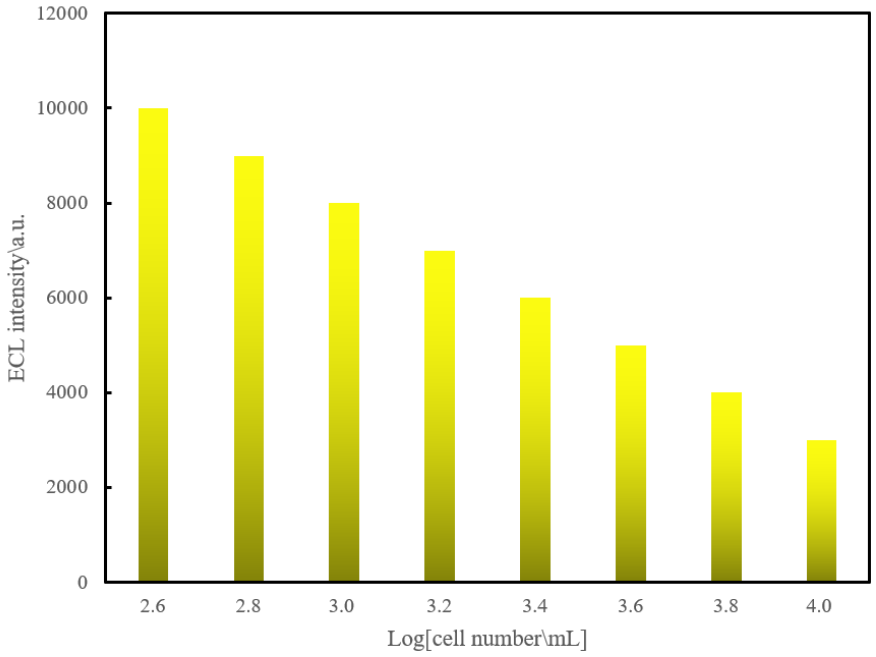


**Figure 9.** Linear data plot of electrochemiluminescence signal intensity vs. logarithm of cell concentration.

### 4.3. Preliminary analysis of actual samples

To further verify the practicability of this sensor, in this paper, the encapsulated sensor was applied to detect human serum samples containing a certain concentration of human hepatoma cells (HepG2) (see **Table 1**). And compared with the traditional enzyme-linked immunosorbent assay. It can be seen that the relative standard deviation of the detection results of these two methods is within 8%. Although this

biosensor is not the best method to directly detect liver cancer cells, it will show great potential in future clinical applications.

**Table 1.** Concentration of cells in serum determined using this design and enzyme-linked immunosorbent assay.

| | ELISA method [cell/mL] | Designed sensor [cell/mL] | Relative standard deviation [%] |
|---|---|---|---|
| Sample 1 | 509 | 578 | 5.36 |
| Sample 2 | 823 | 788 | 4.15 |
| Sample 3 | 5833 | 6039 | 6.58 |
| Sample 4 | 8056 | 8755 | 7.42 |

### 4.4. Evaluation of sensor specificity and anti-interference ability

While the sensor showed good selectivity in comparison to HeLa cells, its specificity in distinguishing closely related cell types or biomarkers was also tested in order to evaluate its potential for application in complex biological environments. The results show that the sensor performs significantly differently in a variety of different cell types and is able to effectively differentiate between closely related biomarkers. This feature enables the sensor to exhibit wider applicability in complex biological environments.

The ability to resist interference in complex biological matrices is also a key factor in evaluating the reliability of biosensors. This paper conducts detailed testing of the sensor's performance in different biological matrices and adopts a series of measures to reduce interference from other biomolecules or compounds. These measures include optimizing sensor surface chemical modifications to improve selective recognition capabilities, and multiple control experiments to exclude non-specific signals. The results show that the sensor can still maintain high selectivity and stability in complex environments.

## 5. Discussion

With the continuous development of life science, people have higher and higher demands for the analysis and detection of life-related proteins, small molecules and toxic environmental pollutants. In order to obtain complete life information, it is urgent to develop some analytical and detection methods with high sensitivity, good selectivity, simple operation and low cost.

Electrochemiluminescence (ECL) is a new analytical method developed for the interaction of chemiluminescence and electrochemistry. When a certain voltage or current is applied to the electrode surface, a chemical reaction occurs between the reaction electrodes or between some components of the reaction electrode product and the solution, resulting in an excited state.

In recent years, nanomaterials with special properties have been applied in various fields. The application of nanomaterials into biosensors opens up a very valuable new way of studying biosensors. The most representative ones are the application of graphene nanomaterials and gold nanomaterials in biosensors. The main purpose of the ECL biosensor based on nanocomposite materials studied in this paper is to solve the problem of accurate, fast, simple and low-cost detection of cells.

During the development of a sensor, not only its technical performance needs to

be considered, but its economic feasibility and market potential also need to be assessed. Cost-benefit analysis shows that the sensor has low production costs and has the potential to achieve large-scale production. According to market analysis, sensors have broad application prospects in the medical detection market. At the same time, the development process strictly follows relevant regulatory requirements to ensure that the sensor meets medical device standards, especially in terms of biocompatibility and safety, to ensure its compliance in clinical applications.

In order to ensure the reliability of the model, this paper conducts detailed verification on a large amount of experimental data. Through multiple experiments and repeated tests, the experimental data collected comprehensively covered the performance of the sensor under various conditions. The results show that the model exhibits a high degree of consistency under a variety of experimental conditions, verifying the accuracy of the theoretical data and the practicability of the model. These experimental data provide solid support for the model proposed in this article and significantly enhance the credibility of the research results.

The use of nanomaterials in biosensor development raises potential ethical and safety issues, especially for in vivo applications. This article conducts an in-depth discussion on this issue, analyzes the potential risks of nanomaterials in in vivo and in vitro applications, and proposes corresponding safety assessment strategies. These strategies include biocompatibility testing of nanomaterials, analysis of potential toxicity, and strict regulatory compliance requirements to ensure the safe application of nanomaterials in biosensors.

## 6. Conclusions

This paper combines biosensors and carbon nanotechnology. A series of nanocomposites have been prepared using various methods. It involves noble metals, metal oxides, carbon-based materials, quantum dots, conductive polymers, etc., and uses SEM, TEM, XRD and other technical means to characterize the appearance, morphology and structural composition of the materials. The fabricated nanocomposites were then further applied to construct sensors. Research shows that for electrochemical enzyme sensors, nanomaterials can effectively enhance electron transfer between enzyme molecules and electrodes. For the enzyme-free electrochemical sensor, the nanomaterial-modified glassy carbon electrode showed good electrocatalytic performance for the target detection substance, and all achieved ideal results. In this study, the synthesis technology of nanocomposite materials and the theory of biosensor theory were deeply studied, and an electrochemiluminescence sensor was designed. The author also conducts experimental research on it, which shows that the development of new nanomaterials and the improvement of sensor technology have certain reference significance.

**Author contributions:** Conceptualization, MW and NJ; methodology, MW; software, MW; validation, MW and NJ; formal analysis, MW; investigation, MW; resources, NJ; data curation, MW; writing—original draft preparation, MW; writing—review and editing, NJ; visualization, MW; supervision, NJ; project administration, MW; funding acquisition, NJ. All authors have read and agreed to the published version of the

manuscript.

**Ethical approval:** Not applicable.

**Conflict of interest:** The authors declare no conflict of interest.

## References


1. Wang K, Wang H, Cheng YB. Large-scale synthesis of α-Si3N4 nanofibers and nanobelts from mesoporous silica-carbon nanocomposites. Journal of Ceramic Science and Technology. 2017; 8(2): 259–264.
2. Bagotia N, Choudhary V, Sharma DK. Studies on toughened polycarbonate/multiwalled carbon nanotubes nanocomposites. Composites Part B: Engineering. 2017; 124: 101–110. doi: 10.1016/j.compositesb.2017.05.037
3. Liang J, Chen J, Shen H, et al. Hollow Porous Bowl-like Nitrogen-Doped Cobalt/Carbon Nanocomposites with Enhanced Electromagnetic Wave Absorption. Chemistry of Materials. 2021; 33(5): 1789–1798. doi: 10.1021/acs.chemmater.0c04734
4. Jang KS, Yeom HY, Park JW, et al. Morphology, electrical conductivity, and rheology of latex-based polymer/nanocarbon nanocomposites. Korea-Australia Rheology Journal. 2021; 33(4): 357–366. doi: 10.1007/s13367-021-0028-7
5. Kozlov GV, Dolbin IV. Fractal Treatment of Melt Viscosity of Polypropylene/Globular Carbon Nanocomposites. Journal of Engineering Thermophysics. 2021; 30(1): 163–169. doi: 10.1134/s1810232821010124
6. Wang F, Zhao Z, Hao C, et al. Enhanced Lithium Storage Property Boosted by Hierarchical Hollow-Structure WSe2 Nanosheets/N, P-Codoped Carbon Nanocomposites. ACS Applied Energy Materials. 2021; 4(10): 11643-11651. doi: 10.1021/acsaem.1c02382
7. Li Y, Zhou P, An F, et al. Dynamic Self-Stiffening and Structural Evolutions of Polyacrylonitrile/Carbon Nanotube Nanocomposites. ACS Applied Materials & Interfaces. 2017; 9(6): 5653–5659. doi: 10.1021/acsami.6b16029
8. Pal R, Jha AK, Akhtar MJ, et al. Enhanced microwave processing of epoxy nanocomposites using carbon black powders. Advanced Powder Technology. 2017; 28(4): 1281–1290. doi: 10.1016/j.apt.2017.02.016
9. Nahm KS. Synthesis and Electocatalytic Activity of MnO2/RuO2/Carbon Nanocomposites to Enhance Lithium-Oxygen Battery Performance. ECS Meeting Abstracts. 2020; MA2020-02(2): 385–385. doi: 10.1149/ma2020-022385mtgabs
10. Li S, Dong B, Yuanyuan, et al. Synthesis of Porous Mo2C/Nitrogen—Doped Carbon Nanocomposites for Efficient Hydrogen Evolution Reaction. ChemistrySelect. 2020; 5(45): 14307–14311. doi: 10.1002/slct.202003639
11. Shabanova IN, Kodolov VI, Terebova NS. X-Ray Photoelectron Study of the Formation of the Chemical Bond and the Atomic Magnetic Moment in Nickel-Carbon Nanocomposites Modified by d-Metal Oxides. Journal of Surface Investigation: X-ray, Synchrotron and Neutron Techniques. 2020; 14(6): 1139-1143. doi: 10.1134/s1027451020060154
12. Song J, Guo S, Ren D, et al. Rice husk-derived SiOx@carbon nanocomposites as a high-performance bifunctional electrode for rechargeable batteries. Ceramics International. 2020; 46(8): 11570-11576. doi: 10.1016/j.ceramint.2020.01.185
13. Wu L, Zhang X, Anthony Thorpe J, et al. Mussel-inspired polydopamine functionalized recyclable coconut shell derived carbon nanocomposites for efficient adsorption of methylene blue. Journal of Saudi Chemical Society. 2020; 24(8): 642–649. doi: 10.1016/j.jscs.2020.07.002
14. Bondarenko LS, Magomedov IS, Terekhova VA, et al. Magnetite-Activated Carbon Nanocomposites: Synthesis, Sorption Properties, and Bioavailability. Russian Journal of Applied Chemistry. 2020; 93(8): 1202-1210. doi: 10.1134/s1070427220080133
15. Shi H, Liu L, Shi Y, et al. Silicon monoxide assisted synthesis of Ru modified carbon nanocomposites as high mass activity electrocatalysts for hydrogen evolution. International Journal of Hydrogen Energy. 2019; 44(23): 11817-11823. doi: 10.1016/j.ijhydene.2019.03.042
16. Sultana I, Rahman MM, Liu J, et al. Antimony-carbon nanocomposites for potassium-ion batteries: Insight into the failure mechanism in electrodes and possible avenues to improve cyclic stability. Journal of Power Sources. 2019; 413: 476-484. doi: 10.1016/j.jpowsour.2018.12.017
17. Alhan S, Nehra M, Dilbaghi N, et al. Potential use of ZnO@activated carbon nanocomposites for the adsorptive removal of Cd2+ ions in aqueous solutions. Environmental Research. 2019; 173: 411-418. doi: 10.1016/j.envres.2019.03.061
18. Kataria N, Garg VK. Application of EDTA modified Fe3O4/sawdust carbon nanocomposites to ameliorate methylene blue and brilliant green dye laden water. Environmental Research. 2019; 172: 43-54. doi: 10.1016/j.envres.2019.02.002
19. Muratov DG, Vasilev AA, Efimov MN, et al. Metal-Carbon Nanocomposites FeNi/C: Production, Phase Composition,

Magnetic Properties. Inorganic Materials: Applied Research. 2019; 10(3): 666-672. doi: 10.1134/s2075113319030298
20. Nita C, Fullenwarth J, Monconduit L, et al. Influence of carbon characteristics on Sb/carbon nanocomposites formation and performances in Na-ion batteries. Materials Today Energy. 2019; 13: 221-232. doi: 10.1016/j.mtener.2019.05.009
21. Ren J, Liu Y, Kaplan DL, et al. Interplay of structure and mechanics in silk/carbon nanocomposites. MRS Bulletin. 2019; 44(1): 53-58. doi: 10.1557/mrs.2018.320
22. Kodolov V, Trineeva V, Lapin A, et al. Characteristics of metallo-carbon nanocomposites in perspective of use in living systems. Morphological Newsletter. 2018; 26(1): 46-51.